

3D magnetic inversion in highly magnetic environments using an octree mesh discretization

Kristofer Davis

UBC-Geophysical Inversion Facility
Dept. of Ocean and Earth Sciences
University of British Columbia
6449 Stores Rd
Vancouver, BC V6T 1Z4, Canada
kdavis@eos.ubc.ca

Douglas W. Oldenburg

UBC-Geophysical Inversion Facility
Dept. of Ocean and Earth Sciences
University of British Columbia
6449 Stores Rd
Vancouver, BC V6T 1Z4, Canada
doug@eos.ubc.ca

SUMMARY

Standard techniques for inverting magnetic field data are marginalized when the susceptibility is high and when the magnetized bodies have considerable structure. A common example is a Banded Iron Formation where the causative body is highly elongated, folded, and has susceptibility greater than unity. In such cases the effects of self-demagnetization must be included in the inversion, which can be accomplished by working with the full Maxwell's equations for magnetostatic fields. This problem has previously been addressed in the literature but there are still challenges with respect to obtaining a numerically robust and efficient inversion algorithm. In our paper we use a finite volume discretization of the equations and an adaptive octree mesh. The octree mesh greatly reduces the number of active cells compared to a regular mesh, which leads to a decrease of the storage requirement as well as a substantial speed up of the inversion. Synthetic and field examples are presented to illustrate the effectiveness of our method.

Key words: self-demagnetization, inversion, magnetics, octree, Maxwell's equations

INTRODUCTION

Magnetic data are often collected over causative bodies in mineral exploration applications. A common assumption for inversion techniques is that the susceptibility of the body is well below 0.1 SI. Highly-susceptible elongated source bodies can be affected by self-demagnetization. This occurs when the neighbouring magnetic domains within the body affect the direction and strength of the local inducing field. (Clark and Emerson, 1999). Self-demagnetization is often present in kimberlite pipes, nickel deposits, unexploded ordnance, and Banded Iron Formations (e.g. Wallace, 2006). In these circumstances the assumption of small susceptibilities is no longer valid ignoring them in the inversion can lead to poor inversion results

Considerable literature has been devoted to remanent magnetization and the estimation of its direction (e.g. Paine *et al.* 2001; Phillips, 2003; Li *et al.* 2004; Dannemiller and Li, 2006) but much less attention has been paid to self-demagnetization. One approach, developed by Shearer (2006), has its roots in the the remanent magnetization

problem. The technique solves for the amplitude of the magnetic field; a quantity weakly dependent upon magnetization direction. The result is a recovered model of 3D varying distribution of susceptibility. Krahenbuhl and Li (2007) showed the method's utility to the self-demagnetization problem. A more rigorous approach is to use integral equation techniques. Another approach, and the one adopted in this paper, is the technique of Lelièvre and Oldenburg (2009). They solve for the full Maxwell's equations for source-free magnetostatics using a finite volume discretization. The innovation here is to modify the methodology to incorporate an octree discretization. This reduces the size of the problem and introduces considerable flexibility to model small scale tortuous bodies in a large volume (e.g. Haber, 2001, Davis and Li, 2010).

In this paper we briefly discuss the governing equations and finite volume discretization method as it applies to the octree discretization. Results of the forward modelling are presented as well as our inversion methodology. Finally we discuss practical aspects for improving speed and robustness during the process of minimization.

FORWARD MODELLING

Maxwell's equations for a static field with no source are:

$$\nabla \cdot \mathbf{B} = 0 \quad (1)$$

$$\nabla \times \mathbf{H} = 0 \quad (2)$$

where \mathbf{H} is the magnetic field strength and \mathbf{B} is the magnetic flux density and is related to the magnetic field through the constitutive relation

$$\mathbf{B} = \mu \mathbf{H}, \quad (3)$$

where μ is a scalar magnetic permeability. This relationship is valid for any magnetically isotropic and linear medium. The magnetic field strength can be expressed as the gradient of the potential, φ :

$$\mathbf{H} = \nabla \varphi. \quad (4)$$

The magnetic permeability, μ , is related to the magnetic susceptibility, χ , by

$$\mu = \mu_0 (1 + \chi), \quad (5)$$

where μ_0 is the magnetic permeability of free space. When the susceptibility is much smaller than unity, the permeability is almost equal to that of free space and the local magnetization will be in the same direction as the inducing field. This assumption forms the basis of most inversion algorithms used in mineral exploration (e.g. Li and Oldenburg, 1996).

The combination of Equations 1, 3 and 4

$$\nabla \cdot \mu \nabla \phi = 0. \quad (6)$$

Solutions for equation 6 have been studied extensively for the methods of finite element and finite volume. We use a finite volume discretization on an octree mesh (Haber *et al.* 2007). Our equations are

$$\mathbf{B} = \mu \nabla \phi, \quad (7)$$

$$\nabla \cdot \mathbf{B} = 0, \quad (8)$$

Each cell in our volume of interest has a constant permeability, μ . The potentials, ϕ , are placed at the cell centres and the unknown flux values, \mathbf{B} , are assigned to the centres of the cell faces. Figure 1 illustrates the positioning of the unknown variables for a single discretized cell. A right-hand rule with z-vertical downward is adopted.

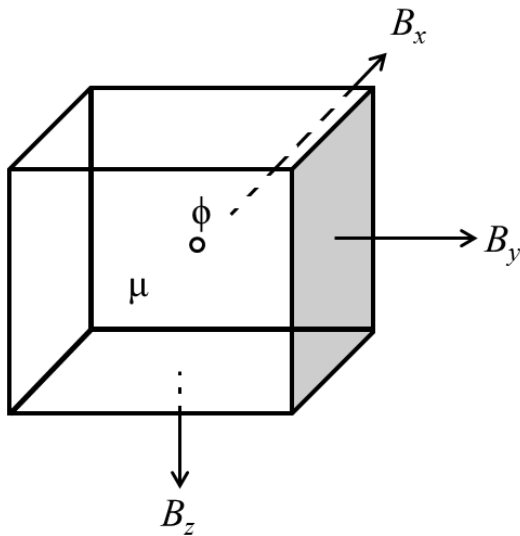


Figure 1. The placement of unknown variables for a single cell. The right-hand rule with z-vertical down is used.

In a finite volume method, the equations are integrated over cells and the matrix-vector system corresponding to Equations 8 and 9 and discretization is carried out creating the system of equations

$$\mathbf{DB} = \mathbf{q}, \quad (9)$$

$$\mathbf{B} = \mathbf{XG}\phi, \quad (10)$$

where \mathbf{G} is the gradient operator, \mathbf{D} is the divergence operator, \mathbf{X} is a diagonal matrix of harmonically averaged permeability values and \mathbf{q} contains non-zero elements due to boundary conditions. The harmonic averaging is required to satisfy the continuity of \mathbf{B} across cell faces. Equations 9 and 10 are combined to create the final equation

$$\mathbf{DXG}\phi = \mathbf{q}. \quad (11)$$

Working with the total flux can be difficult because the anomalous fluxes in which we are interested are much smaller than that due to the primary field. To avoid machine precision problems, a secondary flux formulation is employed. The anomalous flux, \mathbf{B}_s , and anomalous potential ϕ_s , are defined as

$$\mathbf{B}_s = \mathbf{B} - \mathbf{B}_0, \quad (12)$$

$$\phi_s = \phi - \phi_0. \quad (13)$$

The above equations can be combined with Equations 9 and 10 to form the discrete system for the secondary flux formulation:

$$\mathbf{B}_s = (\mu_0^{-1} \mathbf{X} - \mathbf{I}) \mathbf{B}_0 + \mathbf{XG}\phi_s, \quad (14)$$

$$\mathbf{DB}_s = \mathbf{q}_s = \mathbf{q} - \mathbf{DB}_0, \quad (15)$$

where \mathbf{I} is the identity matrix and \mathbf{q}_s are the non-zero elements from the secondary fluxes. The non-zero vector allows for the boundary to be large when the secondary fluxes are significant. The general problem of forward modelling takes the form

$$\mathbf{A}(\mathbf{m})\phi_s = \mathbf{b}(\mathbf{m}). \quad (16)$$

The secondary scalar potentials are solved via a bi-conjugate gradient stabilized (e.g. Saad 1996) algorithm with an incomplete LU-decomposition to aid in convergence. The anomalous flux values are calculated from the recovered potentials and ultimately interpolated to the data locations.

One important aspect of the finite volume discretization is the level of accuracy that is dependent upon the cell size and average permeability values. To increase accuracy in regions of high permeability contrast and tortuous structure, we need to work with small cells; however that can lead to excessively large problems. To handle such problems we use a semi-unstructured mesh. An octree-based discretization is utilized to create small cells where accuracy is more important and coarser cells elsewhere. This decreases the amount of storage required for the modelling and inversion.

OCTREE DISCRETIZATION

Octree discretization is an approach that creates a semi-structured grid in order to preserve accuracy yet decrease the amount of computation storage required. For linear problems, octrees are determined prior to calculating the kernel functionals because the forward modelling requires only matrix-vector operations. Adaptive discretization can significantly reduce the storage requirement for non-linear methods through multi-grid methods (e.g. Haber *et al.* 2007). Octrees are based on hierarchical structure and require the finest possible mesh to be dimensions of $2^i \times 2^j \times 2^k$. The mesh begins coarse, splitting cells into quadrants as required based on a given threshold value. The mesh is regularized so that every cell either has one or two neighbours for every direction. We choose a hybrid approach by applying an octree

discretization based on prior information, such as topography and geology, and then perform minor updates to the mesh based on flux values as necessary. If no geologic information is available the mesh is discretized coarsely except in areas of high topographic relief. A proxy of the subsurface based on transformations of the observed magnetic anomaly have also been shown to be useful in adaptive staggered-grid mesh discretization (e.g. Davis and Li, 2011).

The flux values are then located on the centre of each cell face. For large cells, ghost points for two faces are used in order to properly assign the flux to the surrounding cells. This also ensures that the discretization remains accurate to the second order. Figure 2 is an illustration in two dimensions for simplicity. The geometry between the four small cells on the right of Figure 2 remains the consistent with Figure 1.

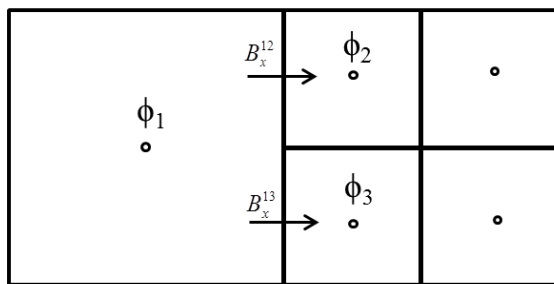


Figure 2. A 2D example showing the representation of flux over multiple faces for large for a single cell. The discretization is regularized such that cells can only have one or two neighbours.

We use a tabular body for an example of octree discretization. The body is shown in Figure 3a. A cross-section of a full octree mesh based on the prior knowledge is presented in Figure 3b. The minimum cell dimensions are 10 x 10 x 10 m. The full mesh contains 1,048,576 number of cells, and working on this mesh requires solving for 1,048,576 potentials and 3,112,960 fluxes. In the octree-based mesh only 17,350 potentials and 56,144 flux values need to be found to complete the solution for the forward problem. The current example is a work in progress, but the accuracy of the forward problem will remain the same yet require approximately 50 times less disk storage. For illustration anomalous data maps based on the tabular body for the full and octree mesh, respectively are presented in Figures 4a and 4b. Although this is an extreme case where we assume the geology is known, an adaptive mesh can allow the inversion and modelling of large-scale datasets in high-susceptibility environments where the size of the full solution can render the problem intractable.

INVERSION

The inversion of an adaptive octree-based model mesh is straightforward once the neighbouring cells are established. The discretized earth contains m prisms with a constant susceptibility, χ . The problem is formulated as an optimization in which we minimize a global objective function consisting of a data misfit function and model objective function. The data misfit function quantifies how well the forward problem reproduces the observed data. The model objective function quantifies the model smoothness through the derivatives of the model and can incorporate a reference model if desired. The

model objective function is calculated on the octree mesh. As one would expect, this step is not as straightforward as it would be with a regular mesh. However, the required knowledge of the neighbouring cells for the anomalous magnetic fluxes creates a convenient parallel in order to calculate the model weighting matrix. A Gauss-Newton approach is used to minimize the total objective function.

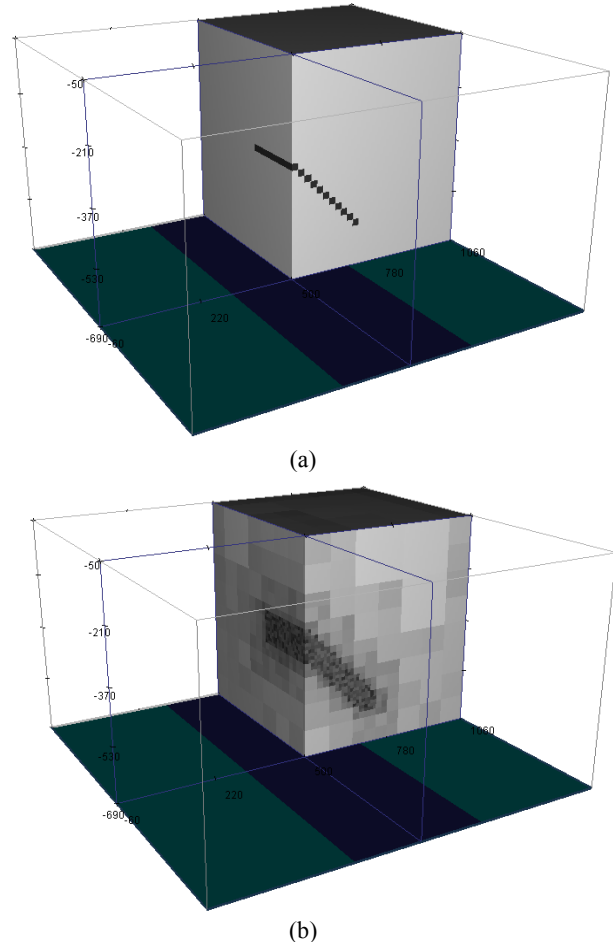


Figure 3. A dipping tabular body (a) used as an illustration for octree discretization. With prior knowledge, the mesh is gridded via octree discretization (b) so that the smallest cell dimensions are in the location of the anomalous body via octrees. The smaller cell sizes are in darker colours.

PRACTICAL APPLICATION

Positivity is required for the recovery of a geologically appropriate susceptibility model. The method of Lelièvre and Oldenburg (2009) redefines the model as the square-root of susceptibility. The advantage to this is that high susceptibilities and discontinuities are not penalized through the model objective function. Unfortunately, this is done at the cost of extra terms in the approximate Hessian during the Gauss-Newton minimization. Less accurate approximate Hessian can affect the convergence of the minimization. Furthermore, the initial model given in terms of square roots requires large values to avoid the problem of a dramatic increase in number of iterations to minimize the global objective function. We choose to use a projected-gradient approach for the solution of $\delta\mathbf{m}$ during the Gauss-Newton

iterations. The use of the projected gradients enforces positivity with the added benefit of speed versus conjugate gradients.

Lastly, a distance weighting is applied to offset the natural decay of the kernel function (Li and Oldenburg, 1996). The weighting is based on the distance of each cell centre to each observation location. The locations of the cell centres are required for the forward modelling of the potentials and are also used in the calculation of the weighting function.

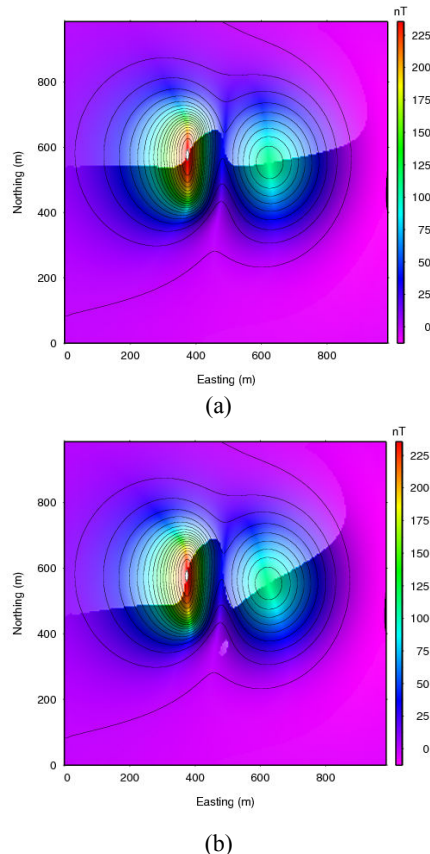


Figure 4. Data maps created by the full (a) and the octree (b) mesh discretization for a tabular body of $SI=1.0$.

CONCLUSIONS

We have incorporated an octree-based mesh for the inversion of magnetic data in high susceptibility environments. Standard methods for inverting data in these cases may be problematic. Therefore, our approach works with the full Maxwell's equations for magnetostatic fields. The discretization greatly reduces the number of model parameters required and can increase accuracy of the forward problem which is dependent upon cell size. Use of projected gradient allows us to directly solve for susceptibility and enforce positivity. Synthetic and field forward modelling and inversion examples are presented to illustrate the effectiveness of the method.

ACKNOWLEDGMENTS

We thank Eldad Haber for helpful discussions on the octree discretization.

REFERENCES

- Clark, D. A. and D. W. Emerson, 1999, Self-demagnetization: Preview, Apr/May, 22–25.
- Dannemiller, N. and Y. Li, 2006, A new method for estimation of magnetization direction: *Geophysics*, 71, L69-L73.
- Davis, K. and Y. Li, 2011, Fast solution of geophysical inversion using adaptive mesh, space-filling curves and wavelet compression: *Geophysical Journal International*, 185, 157-166.
- Davis, K. and Y. Li, 2010, Efficient 3D inversion of magnetic data via octree mesh discretization, space-filling curves, and wavelets: *SEG Expanded Abstracts*, 29, 1172-1177.
- Haber, E., 2001, A mixed finite element method for the solution of the magnetostatic problem with highly discontinuous coefficients: *Computational Geosciences*, 4, 56-71.
- Haber, E., S. Heldmann, and U. Ascher, 2007, Adaptive finite volume method for distributed non-smooth parameter identification, *Inverse Problems*, 23.
- Krahenbuhl, R. A. and Y. Li, 2007, Influence of self-demagnetization effect on data interpretation in strongly magnetic environments: 19th International Geophysical Conference and Exhibition, Perth, WA, Extended Abstracts.
- Li, Y., S. E. Shearer, M. Haney, and N. Dannemiller, 2004, Comprehensive approaches to the inversion of magnetic data with strong remanent magnetization: *SEG Expanded Abstracts* 23, 1191.
- Li, Y., and D. W. Oldenburg, 3-D inversion of magnetic data: *Geophysics*, 61, 394-408.
- Lelièvre, P. G. and D. W. Oldenburg, 2009, Magnetic forward modelling and inversion for materials of high susceptibility: *Geophysical Journal International*, 166, 76-90.
- Paine, J., Haederle, M., and Flis, M., 2001, Using transformed TMI data to invert for remanently magnetized bodies: *Exploration Geophysics*, 32, 238-242.
- Phillips, J.D., 2003, Can we estimate total magnetization directions from aeromagnetic data using Helbig's formulas: IUGG 2003 - Abstracts Week B, p.B261 and IUGG 2003 Program and Abstracts CDROM
- Saad, Y., 1996, Iterative methods for sparse linear systems, PWS Publishing, Boston, Massachusetts, USA.
- Shearer, S. E., 2006, 3-D inversion of magnetic data in the presence of remanent magnetization: MS Thesis, Colorado School of Mines, Golden, Colorado USA.
- Wallace, Y., 2006, 3D modeling of banded iron formation incorporating demagnetization – A case study at the Musselwhite Mine, Ontario, Canada: AESC 2006, Melbourne, Australia.